Integrated 1 × 8 Optical Phased-Array Switch With Low Polarization Sensitivity for Broadband Optical Packet Switching
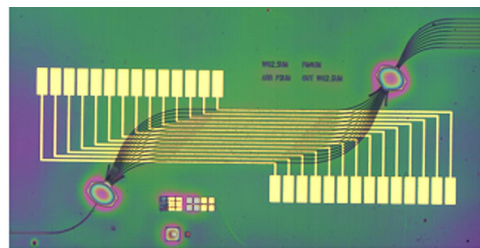
Ibrahim Murat Soganci, Student Member, IEEE
Takuo Tanemura, Member, IEEE
Yoshiaki Nakano, Member, IEEE

Integrated 1 × 8 Optical Phased-Array Switch With Low Polarization Sensitivity for Broadband Optical Packet Switching

Ibrahim Murat Soganci, *Student Member, IEEE*,
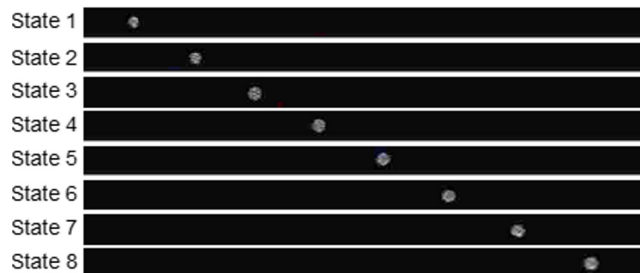**Takuo Tanemura, *Member, IEEE*, and Yoshiaki Nakano, *Member, IEEE***

Research Center for Advanced Science and Technology, University of Tokyo, Tokyo 153-8904, Japan

Abstract: An InP/InGaAsP integrated 1 × 8 optical phased-array switch is designed, fabricated, and characterized for high-throughput broadband wavelength-division multiplexed (WDM) optical packet switching application. With a single stage of phase shifters utilizing carrier-induced refractive index change, switching to the eight output ports is demonstrated successfully. The polarization-dependent loss is 2.2 dB in the worst case, and the wavelength-dependent loss is less than 2.5 dB across the entire *C*-band (1520–1580 nm) with the average extinction ratio of 17.7 dB. The measured reconfiguration time is shorter than 6 ns. Low-penalty transmission of a 40-Gb/s non-return-to-zero signal is also demonstrated for the first time. These features make the integrated phased-array switch an attractive candidate to be deployed in the future high-capacity optical packet switching networks.

Index Terms: Advanced optics design, electro-optical systems, fiber optics systems, waveguide devices.

1. Introduction

The growth of capacity requirement in communication networks is expected to increase the power consumption and cost of optical networks with electronic switching nodes. In high-capacity wavelength-division multiplexing (WDM) networks, broadband optical switches, ensuring perfect transparency in both the bit rate and modulation format of the data signal, would potentially offer lower power consumption and cost compared with electronic routers [1], [2]. Optical packet switching (OPS), which offers the highest temporal granularity, is particularly attractive in terms of network utilization efficiency and latency [3]. The OPS technologies require switch fabrics with reconfiguration time ranging from sub-nanosecond to a few nanoseconds depending on the guard time. Also, the throughput of optical routers, which is expected to be close to 1 Pb/s in 2020 [4], necessitates switches with large number of input and output ports. Broadband operation of such switches is advantageous because OPS with WDM payload offers high-throughput low-latency switching with relatively small number of ports [5], [6].

Among several candidates of optical packet switches, monolithically integrated III–V semiconductor switches have basic advantages, such as integrability with other active and passive optical devices, small footprint, and relatively low power consumption. Conventionally, large-scale III–V semiconductor switch fabrics were fabricated by cascading multiple 1 × 2 and 2 × 2 switches [7]–[9].
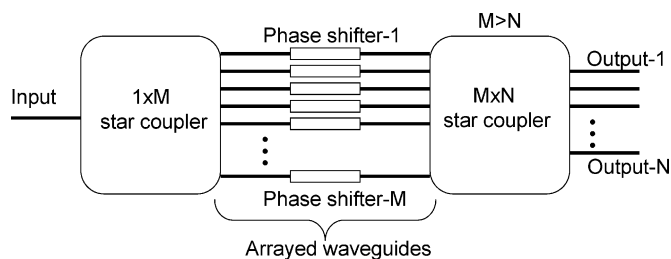
Fig. 1. Schematic diagram of the integrated optical phased-array switch.

However, accumulation of the insertion loss in the switching elements may lead to large optical loss with increasing number of ports. As an alternative approach, broadcast-and-select switches, consisting of passive couplers and semiconductor-optical-amplifier (SOA) gate arrays, have been demonstrated [10]–[12]. The interchannel crosstalks due to gain saturation, optical signal-to-noise ratio (OSNR) degradation, the necessity of active-passive integration, and the relatively high power consumption would be the drawbacks of SOA-based switches.

As an alternative candidate of scalable semiconductor switch, we have recently demonstrated a novel type of integrated high-speed $1 \times N$ switch based on arrayed phase shifters [13]. Unlike cascaded devices, the phased-array switch enables $1 \times N$ switching using a single phase modulation stage, thus offers potential advantages in terms of size and optical insertion loss for large N. Moreover, since the device consists of only phase-modulating sections for switching, it operates with relatively low power consumption, free from excess noise, and does not require active-passive integration, which significantly contributes to the high-yield low-cost fabrication. Our proof-of-concept 1×5 InP switch has demonstrated the potential of wideband operation with nanoseconds dynamic response [13].

Recently, we fabricated an integrated 1×8 switch with the phased-array scheme to experimentally verify the advantages of these switches in terms of scalability. The initial characterization yielded successful results with low wavelength and polarization sensitivity [14]. In this paper, we present the first comprehensive characterization of the integrated 1×8 optical phased-array switch including the wavelength and polarization dependences, dynamic response, and the bit-error-rate (BER) characteristics and investigate the potential applicability of the switch to the broadband WDM OPS routers. We achieve successful switching to all output ports for both the transverse-electric (TE) and transverse-magnetic (TM) polarization states in the spectral band covering the entire *C*-band (1520–1580 nm). The dynamic reconfiguration time is measured to be less than 6 ns, which should be short enough for typical OPS systems. We also demonstrate low-penalty transmission of a 40-Gb/s non-return-to-zero (NRZ) optical signal for the first time. Further issues on performance improvement and scalability are discussed.

2. Design and Fabrication

The integrated optical phased-array switch consists of an input waveguide, two star couplers serving as free propagation regions, several arrayed waveguides with phase shifters and passive output waveguides leading to output ports. A schematic representation of integrated optical switches based on the phased-array scheme is shown in Fig. 1. The optical mode in the input waveguide is diffracted at the first star coupler and couples to the arrayed waveguides. The phase distribution across the array is controlled electrically via the phase shifters attached to each waveguide. The modes from the arrayed waveguides then couple to the second star coupler, which is identical to the first one. The interference pattern at the output plane linearly depends on the phase difference between adjacent arrayed waveguides, so it is possible to switch to any desired output by dynamically controlling the electrical driving conditions of the phase shifters.

The optimized structure of the switch was derived to minimize the device size, while achieving sufficient switching performance [15]. The width of the waveguides was designed to be 2.5 μm at the bends, 4 μm at the phase shifters, and 5 μm at the input and outputs of the device. Linear tapers
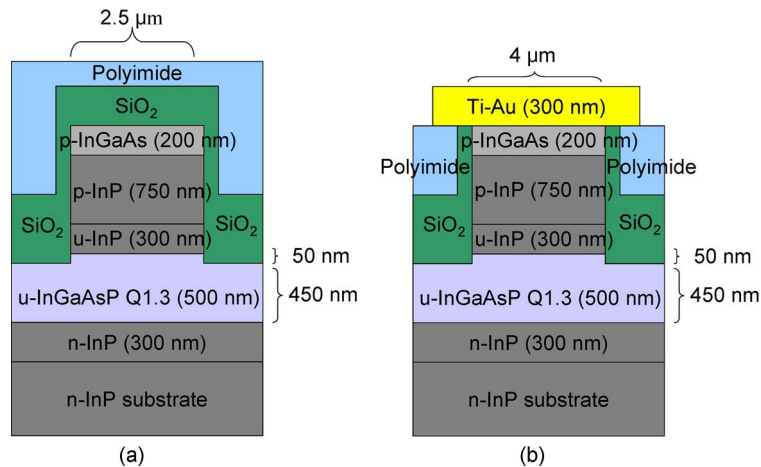
Fig. 2. Schematic cross section of the epitaxial design of (a) passive waveguides and (b) phase shifters.

were used to connect the waveguides with different widths. An anti-symmetrical design was used in the array section to keep all the arrayed waveguides equal in length. This is necessary for broadband switching of WDM signals. The minimum radius of curvature is 360 μm at the bends, which, according to our calculation, leads to negligible bending loss while keeping the device size small. Both star couplers are 163 μm long, which is designed for low optical crosstalk and insertion loss and uniform distribution of power at the output ports. The array pitch is 3 μm and the output pitch is 3.2 μm. The pitch parameters were designed to obtain low crosstalk and high coupling efficiency between the star coupler and waveguides at the same time. We chose the number of arrayed waveguides to be 14, which was optimized to achieve sufficient extinction ratio with moderate device size. The dimensions of the designed 1 × 8 switch are 3.3 mm × 1.8 mm. Further size reduction is possible by using deeply etched waveguides, which should allow both smaller radii of curvature at the bends and shorter length of the star couplers.

The epitaxial design is identical in the entire device. On the top of the n-doped InP substrate and the InP lower cladding layers, there is a 500-nm-thick unstrained bulk InGaAsP guide layer that has an emission peak at 1.3 μm (Q1.3). Undoped and p-doped InP upper cladding layers and a highly p-doped InGaAs contact layer are stacked on the top of the guide layer. The schematic cross sections of guided-wave phase shifters and passive waveguides are displayed in Fig. 2. Under the effective-refractive-index and Fraunhofer-diffraction approximations, we calculate the on-chip loss of the designed 1 × 8 optical switch to be less than 3 dB at all switching states. The calculated crosstalk is lower than −33 dB between output ports at all states.

The switch was fabricated by single-step metal-organic vapor-phase epitaxial (MOVPE) growth followed by optoelectronic device processing. All passive waveguides, phase shifters and star couplers were formed by shallow etching down to the top of the guide layer by inductively coupled-plasma reactive-ion etching (ICP-RIE). The SiO$_2$ and polyimide layers were applied for passivation and planarization, respectively. These dielectric materials were removed from the top of the phase shifters for electrical contact. Ohmic contact to the phase shifters was formed by electron-beam evaporation of Ti and Au, subsequent lift-off, and annealing. The microscope image of a fabricated 1 × 8 optical phased-array switch is shown in Fig. 3. For the experiments, the electrode pads were wire-bonded to a printed circuit board and the device was mounted on a thermally conductive aluminum nitride chip carrier.

The arrayed phase shifters in the device operate via current injection by forward biasing of the p-i-n double hetero-junction. The change of carrier density in the undoped InGaAsP layer causes the modulation of the refractive index due to the bandfilling, free-carrier-plasma and bandgap-shrinkage effects. The former two mechanisms cause the reduction of the refractive index and the latter causes an increase. In our experimental conditions, using an optical signal at 1.55-μm wavelength band, the current injection to each electrode was less than 20 mA. In these conditions, refractive index reduction
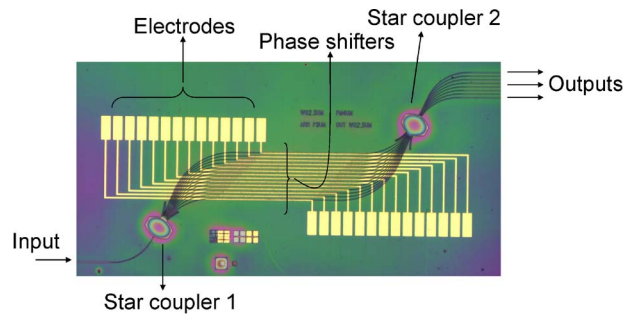
Fig. 3. Micrograph of the fabricated monolithically integrated InP/InGaAsP 1 × 8 optical phased-array switch with 14 arrayed waveguides. The dimensions of the device are 3.3 mm × 1.8 mm. The aberrations at the star couplers are due to the thick polyimide layer.
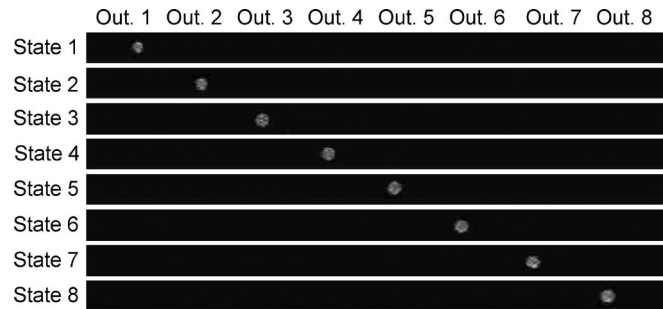

Fig. 4. Infrared camera images at the output of the 1 × 8 optical phased-array switch observed at the eight different switching states (State 1–8). The light is switched to individual output ports (Out. 1–8).

is expected to be dominant for the Q1.3 InGaAsP layer [16]. Due to the 250-nm separation between the signal wavelength and the material bandgap, both the optical loss and dispersion of phase modulation efficiency are low. In addition, these characteristics can be polarization-insensitive in unstrained bulk semiconductors. As a result, we could realize low-loss phase shifters with small wavelength/polarization dependences.

3. Experimental Results and Discussions

We measured the basic static and dynamic characteristics of the fabricated 1 × 8 optical phased-array switch. A wavelength-tunable laser, a variable optical attenuator, polarization controllers, and a lensed optical fiber were used to supply continuous-wave (CW) optical signal at the input of the device. In the static experiments, phase shifters were controlled by a direct current source with multiple channels and the output light was monitored using an optical power meter and an infrared camera. A Peltier cooler was used for temperature stabilization of the device, which was maintained to 20 °C.

Fig. 4 shows the near-field images at the switch output observed at eight different switching states. At each state (State 1–State 8), the light is routed to the corresponding output port (Out. 1–Out. 8), while the signal at the other ports is suppressed. The conditions of phase shifters at different switching states were found using an iterative optimization process, where the peak of optical power was detected while sweeping the current at each phase shifter one by one. The total current injected to the phase shifters was between 50 mA and 95 mA for all cases.

The extinction ratio at all ports was then examined quantitatively by coupling the light from each output port with a lensed fiber and measuring its power. Fig. 5 compares the output power for 8 switching states with TE- and TM-polarized input signal at the wavelength of 1550 nm. For clear view of crosstalk levels, the power is normalized to the best case (State 5, Out. 5, TE), where the fiber-to-fiber loss was measured to be 29.9 dB. The crosstalk suppression ratio is 17.7 dB on average, with 11.5 dB and 10.9 dB in the worst cases for TE- and TM-polarized input, respectively.
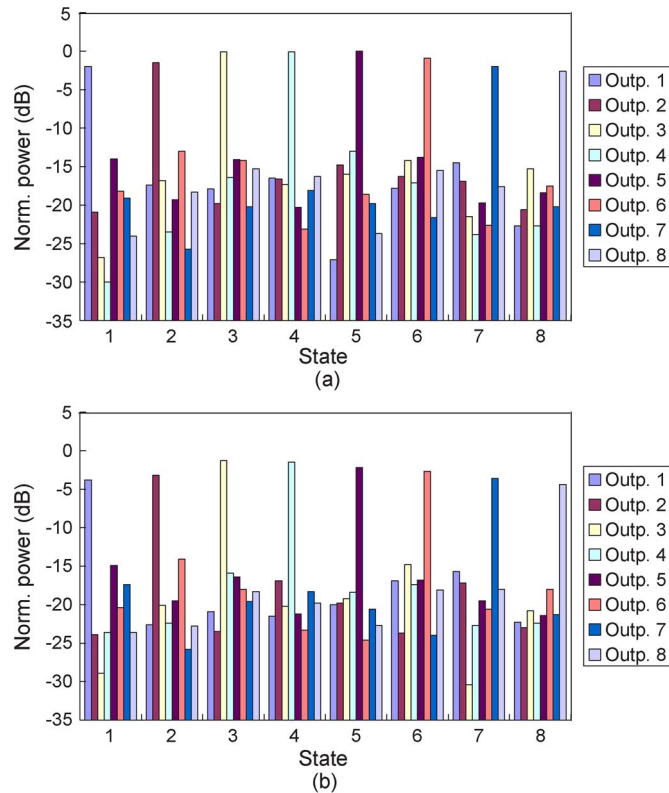
Fig. 5. Comparison of normalized optical power at the output ports of the 1 × 8 optical switch under 8 switching conditions with (a) TE-polarized and (b) TM-polarized CW input signal.

The on/off extinction ratio is larger than 12.1 dB and 11.4 dB for TE- and TM-polarized light, respectively. The polarization-dependent loss (PDL) is in the range of 1.2–2.2 dB at 1550-nm wavelength. It should be noted that during these measurements, the switching conditions were optimized for TE polarization in the beginning and were kept constant without further optimization for TM polarization. We assume that the residual PDL of the switch is mostly caused by the polarization dependence of fiber-to-waveguide coupling efficiency and propagation loss of the waveguides, which should be eliminated by the optimization of the waveguide design and processing.

Among the total fiber-to-fiber loss of 29.9 dB for the best case (State 5, Out. 5, TE), the on-chip loss is estimated to be approximately 18 dB. The major contribution to this loss is the relatively high propagation loss in the waveguides (22–23 dB/cm for TE and 27–28 dB/cm for TM), which can be improved by removing the InGaAs contact layer at the passive sections and with better device processing conditions to reduce sidewall roughness. As mentioned previously, this large polarization-dependent propagation loss is the main contributor to the PDL of the switch. The larger crosstalks in the experiment compared with the calculation are attributed mainly to the fabrication error in the waveguide width, which was confirmed to be up to a few hundred nanometers wider than the designed value. The lithography- and etching-based imperfect waveguide openings of the star couplers and large propagation loss should have also affected the crosstalk characteristics, and should be improved with better processing conditions. In addition, further reduction in crosstalk is expected with appropriate apodization to the interfaces of star couplers, which is a common technique used in arrayed-waveguide gratings. We expect that deterministic control of phase shifters according to the phase error at each arrayed waveguide would also bring better extinction ratio and loss than the existing current sweeping-based iterative algorithm.

We next measured the wavelength dependence of the switch to investigate its applicability in WDM networks. The wavelength of the CW light was swept from 1520 nm to 1580 nm, while the polarization state at the input of the device was changed between TE and TM modes. In Fig. 6, the
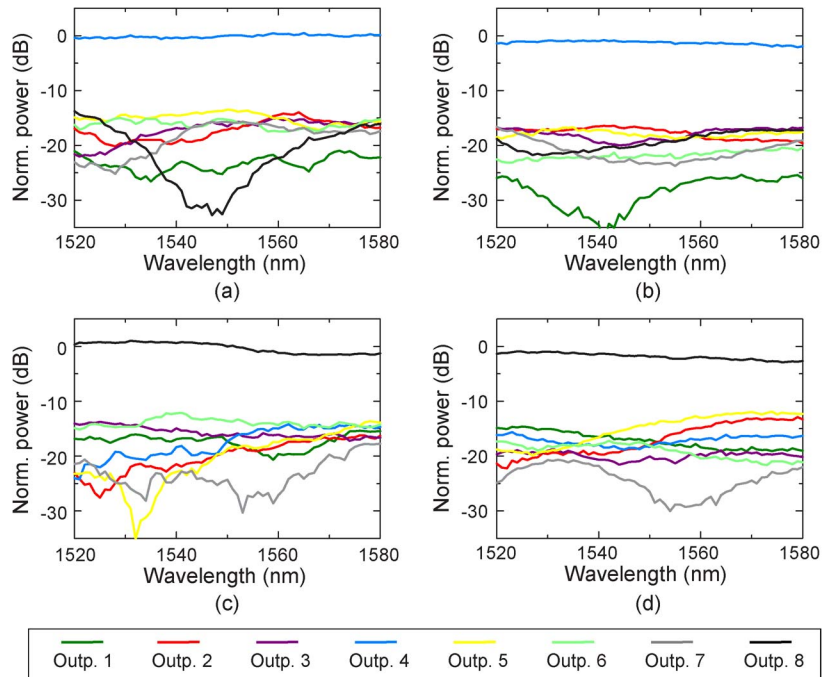
Fig. 6. Normalized optical power at the outputs of the 1 × 8 optical switch as a function of the wavelength at State 4 [TE in (a) and TM in (b)] and State 8 [TE in (c) and TM in (d)]. The normalization was done with respect to the power of 1550-nm-wavelength TE-polarized light at each state.
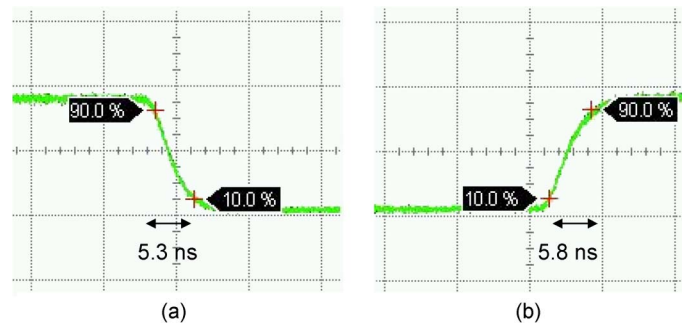

Fig. 7. (a) Falling and (b) rising edges of the optical power at Output 4 in time domain with a square-wave electrical signal applied at one of the phase shifters.

optical power at the output ports at State 4 and State 8 are plotted as a function of wavelength with TE and TM polarization states. Switching is achieved throughout the band for both polarization states at all states with the wavelength-dependent loss lower than 2.5 dB. There is no significant degradation in the crosstalk, which is better than −9.6 dB in the measured wavelength range at State 8. Similar behavior is observed at all switching states. This small wavelength dependence owes to the optimally designed arrayed waveguides with equal path length as well as wavelength-independent operation of the phase shifters.

Additionally, we investigated the dynamic switching response. For simplicity, only one of the phase shifters was driven by a square-wave voltage between 0 V and 1.5 V from an arbitrary waveform generator with 10%–90% transition time of 1.4 ns. All the other electrodes were grounded. Fig. 7 shows the rising and falling edges of the optical waveform from Out. 4 monitored using a high-speed digital sampling oscilloscope with 65-GHz electrical bandwidth. The optical extinction ratio in this measurement is 5.4 dB because only one phase shifter was dynamically driven instead of a complete dynamic switching experiment. The rising edge, which corresponds to
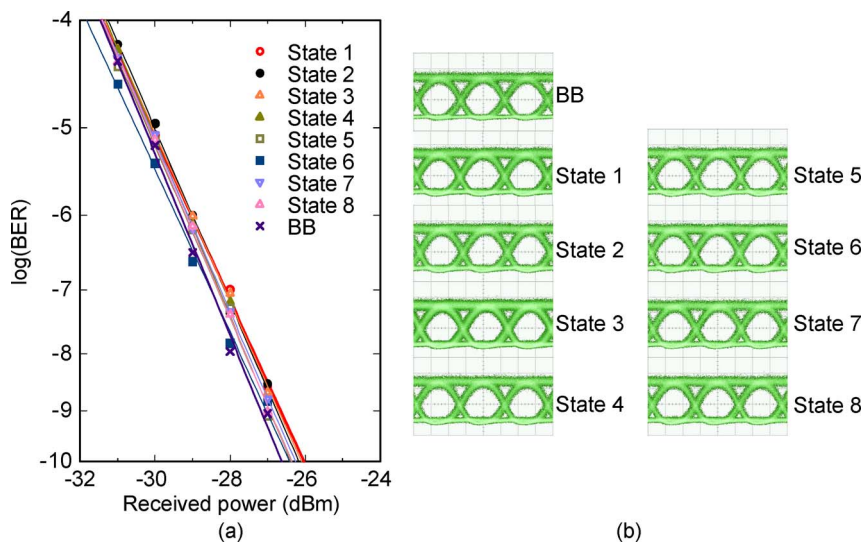
Fig. 8. (a) BER of the 40-Gb/s NRZ-PRBS signal at the switch output for all states (State 1–State 8) and the back-to-back configuration (BB) versus the received optical power and (b) the eye diagrams.

the depletion of carriers, has a 10%-to-90% transition time of 5.8 ns, and the fall time, which corresponds to carrier injection, is 5.3 ns. The measured reconfiguration time should be short enough for typical OPS systems having the guard time of a few nanoseconds. The reconfiguration speed can be limited by the carrier lifetime in the InGaAsP guide layer and/or the electrical parasitics. With the proper design of epitaxial structure and electrical connections, we should be able to achieve sub-nanosecond dynamic response [17]. Moreover, it is also possible to employ the Pockels effect, Franz-Keldysh effect, and/or carrier-depletion effect through reverse-biasing of the p-i-n structure to achieve switching speed beyond the capability of current injection.

Finally, we tested the BER characteristics of the switch with a 40-Gb/s NRZ PRBS optical signal. At each of the 8 states, the BER of optical signal from the corresponding output port was measured in the preamplified receiver configuration. Fig. 8 displays the measured BER versus the received optical power and the corresponding eye diagrams. The power penalty at the BER of 10^{-9} is lower than 0.6 dB at all states. Low-penalty operation is a consequence of the all-passive design of the device.

4. Conclusion

We have designed, fabricated, and characterized a monolithically integrated 1 $\times$ 8 InP/InGaAsP electro-optical phased-array space switch with nanosecond-scale reconfiguration time for the first time. Using the optimally designed array structure and phase shifters, we experimentally obtained 1 $\times$ 8 switching extending beyond the C-band (1520–1580 nm) with the wavelength dependence of 2.5 dB and polarization sensitivity below 2.2 dB. Fast reconfiguration time in the range of 5–6 ns as well as low-penalty transmission of a 40-Gb/s NRZ signal were also demonstrated successfully. With the relatively easy fabrication procedures and the potential scalability of the number of ports, the demonstrated switch is an attractive candidate to be used in the future high-capacity WDM-OPS networks.

References

[1] S. J. B. Yoo, "Optical packet and burst switching technologies for the future photonic Internet," *J. Lightw. Technol.*, vol. 24, no. 12, pp. 4468–4492, Dec. 2006.
[2] E. Bouillet, G. Ellinas, J.-F. Labourdette, and R. Ramamurthy, *Path Routing in Mesh Optical Networks*. Hoboken, NJ: Wiley, 2007.
[3] M. O. Mahony, "Future optical networks," in *Optical Fiber Telecommunications V- B (Systems and Networks)*, I. P. Kaminow, T. Li, and A. E. Willner, Eds. Amsterdam, The Netherlands: Elsevier, 2008.

[4] R. S. Tucker, "The role of optics and electronics in high-capacity routers," *J. Lightw. Technol.*, vol. 24, no. 12, pp. 4655–4673, Dec. 2006.

[5] A. Schaham, B. A. Small, O. L. Ladouceur, and K. Bergman, "A fully implemented 12×12 data vortex optical packet switching interconnection network," *J. Lightw. Technol.*, vol. 23, no. 10, pp. 3066–3075, Oct. 2005.

[6] H. Furukawa, N. Wada, N. Takezawa, K. Nashimoto, and T. Miyazaki, "$640(2 \times 32\lambda \times 10)$ Gbit/s polarization-multiplexed, wide-colored optical packet switching achieved by polarization-independent high-speed PLZT switch," presented at the Optical Fiber Communication Conf., San Diego, CA, 2008, Paper OTuL7.

[7] K. Hamamoto, T. Anan, K. Komatsu, M. Sugimoto, and I. Mito, "First 8×8 semiconductor optical matrix switches using GaAs/AlGaAs electro-optic guided-wave directional couplers," *Electron. Lett.*, vol. 28, no. 5, pp. 441–443, Feb. 1992.

[8] R. Varrazza, I. B. Djordjevic, and S. Yu, "Active vertical-coupler-based optical crosspoint switch matrix for optical packet-switching applications," *J. Lightw. Technol.*, vol. 22, no. 9, pp. 2034–2042, Sep. 2004.

[9] G. Wenger, M. Schienle, J. Bellermann, M. Heinbach, S. Eichinger, J. Muller, B. Acklin, L. Stoll, and G. Muller, "A completely packaged strictly nonblocking 8×8 optical matrix switch on InP/InGaAsP," *J. Lightw. Technol.*, vol. 14, no. 10, pp. 2332–2337, Oct. 1996.

[10] M. Janson, L. Lundgren, A. C. Morner, M. Rask, B. Stoltz, M. Gustavsson, and L. Thylen, "Monolithically integrated 2×2 InGaAsP/InP laser amplifier gate switch arrays," *Electron. Lett.*, vol. 28, no. 8, pp. 776–778, Apr. 1992.

[11] W. van Berlo, M. Janson, L. Lundgren, A.-C. Morner, J. Terlecki, M. Gustavsson, P. Granestrand, and P. Svensson, "Polarization-insensitive, monolithic 4×4 InGaAsP-InP laser amplifier gate switch matrix," *IEEE Photon. Technol. Lett.*, vol. 7, no. 11, pp. 1291–1293, Nov. 1995.

[12] Y. Kai, K. Sone, S. Yoshida, Y. Aoki, G. Nakagawa, and S. Kinoshita, "A compact and lossless 8×8 SOA gate switch subsystem for WDM optical packet interconnections," presented at the European Conf. Optical Communication, Brussels, Belgium, 2008, Paper We.2.D.4.

[13] T. Tanemura, M. Takenaka, A. Al Amin, K. Takeda, T. Shioda, M. Sugiyama, and Y. Nakano, "InP-InGaAsP integrated 1×5 optical switch using arrayed phase shifters," *IEEE Photon. Technol. Lett.*, vol. 20, no. 12, pp. 1063–1065, Jun. 2008.

[14] I. M. Soganci, T. Tanemura, and Y. Nakano, "Polarization-independent broadband 1×8 optical phased-array switch monolithically integrated on InP," presented at the Optical Fiber Communication Conf., San Diego, CA, 2009, Paper OWV1.

[15] T. Tanemura and Y. Nakano, "Design and scalability analysis of optical phased-array $1 \times N$ switch on planar lightwave circuit," *IEICE Electron. Express*, vol. 5, no. 16, pp. 603–609, Aug. 2008.

[16] B. B. Bennett, R. A. Soref, and J. A. Del Alamo, "Carrier-induced change in refractive index of InP, GaAs, and InGaAsP," *IEEE J. Quantum Electron.*, vol. 26, no. 1, pp. 113–122, Jan. 1990.

[17] M. N. Sysak, L. A. Johansson, J. W. Raring, M. Rodwell, L. A. Coldren, and J. Bowers, "A high efficiency, current injection based quantum-well phase modulator monolithically integrated with a tunable laser for coherent systems," presented at the Coherent Optical Technologies and Applications, Whistler, BC, Canada, 2006, Paper CFC6.